Perturbative splitting in DPDs and DPS.

Numerical impact of NLO corrections

November 21, 2023

P. Plößl [1]

[1]Deutsches Elektronen-Synchrotron DESY

Part I

DPDs in the limit of small interparton distance.

Small distance limit of DPDs.

Operator product expansion of DPDs for $\boldsymbol{y} \to 0$:

$$F_{a_1 a_2}(\boldsymbol{y};\mu,\mu) \overset{y\to 0}{=} F^{\text{int}}_{a_1 a_2}(\boldsymbol{y};\mu,\mu) + F^{\text{spl}}_{a_1 a_2}(\boldsymbol{y};\mu,\mu)$$

where $F^{\text{int}}_{a_1 a_2}$ and $F^{\text{spl}}_{a_1 a_2}$ can be expressed in terms of twist-4 distributions and PDFs, respectively.

F^{spl} is enhanced with respect to F^{int} by a factor of $\boldsymbol{y}^{-2}$, making it the leading contribution at small $\boldsymbol{y}$:

$$F_{a_1 a_2}(\boldsymbol{y};\mu,\mu) \overset{y\to 0}{\approx} F^{\text{spl}}_{a_1 a_2}(\boldsymbol{y};\mu,\mu) = \frac{1}{\pi \boldsymbol{y}^2} V_{a_1 a_2, a_0}(\boldsymbol{y},\mu) \underset{12}{\otimes} f_{a_0}(\mu)$$

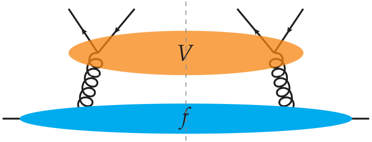

Issues with the DPS cross section?

$$\int \mathrm{d}^2\boldsymbol{y}\, F_{a_1 a_2}(\boldsymbol{y})\, F_{b_1 b_2}(\boldsymbol{y}) \sim \int \frac{\mathrm{d}^2\boldsymbol{y}}{y^4}$$

UV divergent cross section?

Disentangling SPS and DPS.

SPS-DPS ambiguity for contributions of the following form:

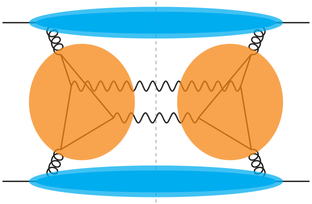

SPS?

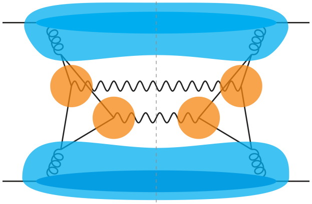

DPS?

Diehl-Gaunt-Schönwald subtraction formalism:

Double counting between SPS and DPS requires a subtraction term:

$$\sigma = \sigma_{\mathrm{SPS}} + \sigma_{\mathrm{DPS}} - \sigma_{\mathrm{sub}}\,, \qquad \sigma_{\mathrm{sub}} = \sigma_{\mathrm{DPS}} \text{ with } F_{ij} \to F_{ij}^{\mathrm{spl}}$$

[Diehl, Gaunt, and Schönwald, 2017]

The UV divergence of the DPS cross section is regulated with a lower cut-off ($y \gtrsim 1/\min(Q_A, Q_B)$).

Disentangling SPS and DPS.

SPS-DPS ambiguity for contributions of the following form:

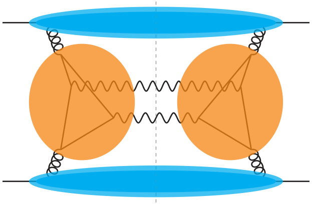

SPS for small y

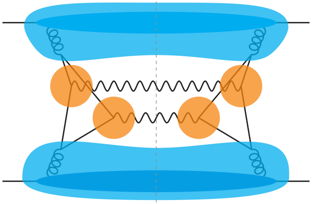

DPS for large y

Diehl-Gaunt-Schönwald subtraction formalism:

Double counting between SPS and DPS requires a subtraction term:

$$\sigma = \sigma_{\text{SPS}} + \sigma_{\text{DPS}} - \sigma_{\text{sub}}\,, \qquad \sigma_{\text{sub}} = \sigma_{\text{DPS}} \text{ with } F_{ij} \to F_{ij}^{\text{spl}}$$ [Diehl, Gaunt, and Schönwald, 2017]

The UV divergence of the DPS cross section is regulated with a lower cut-off ($y \gtrsim 1/\min(Q_A, Q_B)$).

The perturbative $1 \to 2$ splitting at LO.

The $1 \to 2$ splitting kernels can be calculated from Feynman diagrams for partonic DPDs $a_1 a_2$ in a parton a_0:

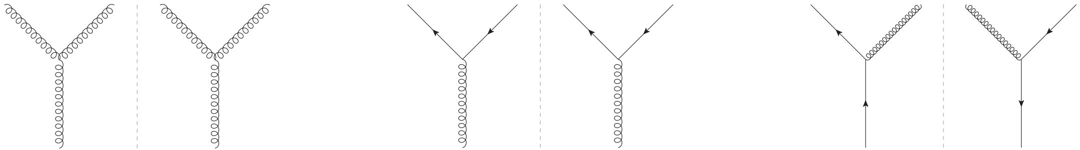

LO splitting formula:

$$F^{\text{spl},\,(1)}_{a_1 a_2}(x_1, x_2, \boldsymbol{y}; \mu, \mu) = \frac{1}{\pi \boldsymbol{y}^2} \frac{\alpha_s(\mu)}{2\pi} V^{(1)}_{a_1 a_2, a_0}\left(\frac{x_1}{x_1+x_2}\right) f_{a_0}(x_1 + x_2; \mu)$$

where:

$$V^{(1)}_{gg,g}(z) = 2\, C_A \left(\frac{1-z}{z} + \frac{z}{1-z} + z(1-z)\right)$$

The perturbative $1 \to 2$ splitting at LO.

The $1 \to 2$ splitting kernels can be calculated from Feynman diagrams for partonic DPDs $a_1 a_2$ in a parton a_0:

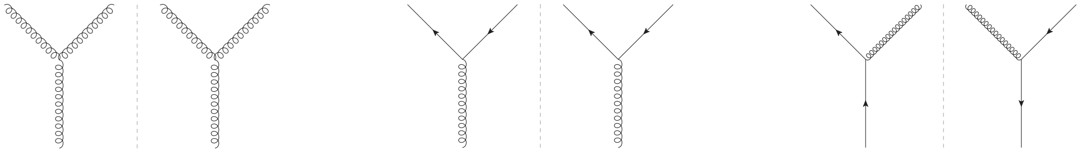

LO splitting formula:

$$F^{\text{spl},(1)}_{a_1 a_2}(x_1, x_2, \boldsymbol{y}; \mu, \mu) = \frac{1}{\pi \boldsymbol{y}^2} \frac{\alpha_s(\mu)}{2\pi} V^{(1)}_{a_1 a_2, a_0}\left(\frac{x_1}{x_1+x_2}\right) f_{a_0}(x_1 + x_2; \mu)$$

where:

$$V^{(1)}_{q\bar{q},g}(z) = T_F \left(z^2 + (1-z)^2\right)$$

The perturbative $1 \to 2$ splitting at LO.

The $1 \to 2$ splitting kernels can be calculated from Feynman diagrams for partonic DPDs $a_1 a_2$ in a parton a_0:

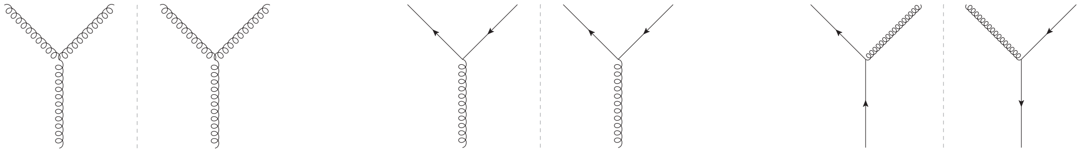

LO splitting formula:

$$F^{\text{spl},(1)}_{a_1 a_2}(x_1, x_2, \boldsymbol{y}; \mu, \mu) = \frac{1}{\pi \boldsymbol{y}^2} \frac{\alpha_s(\mu)}{2\pi} V^{(1)}_{a_1 a_2, a_0}\left(\frac{x_1}{x_1+x_2}\right) f_{a_0}(x_1 + x_2; \mu)$$

where:

$$V^{(1)}_{qg,q}(z) = C_F \frac{1+z^2}{1-z}$$

The “splitting scale”.

At which scale $\mu_{\rm spl}$ should the splitting be evaluated?

The natural scale of the splitting is set by the interparton distance y of the observed partons:

$$\mu_{\rm spl}(y) \sim \frac{1}{y}$$

How to avoid evaluation of the perturbative splitting at non-perturbative scales for large y?

Regularized splitting scale:

$$\mu_{\rm spl}(y) = \frac{b_0}{y^*(y)}\,, \qquad \text{e.g.} \quad y^*(y) = \frac{y}{\sqrt[4]{1 + y^4/y_{\max}^4}}\,, \qquad y_{\max} = \frac{b_0}{\mu_{\min}}$$

The “splitting scale”.

At which scale $\mu_{\rm spl}$ should the splitting be evaluated?

The natural scale of the splitting is set by the interparton distance y of the observed partons:

$$\mu_{\rm spl}(y) \sim \frac{1}{y}$$

How to avoid evaluation of the perturbative splitting at non-perturbative scales for large y?

Regularized splitting scale:

$$\mu_{\rm spl}(y) \approx \frac{1.123}{y^*(y)}\,, \qquad \text{e.g.} \quad y^*(y) = \frac{y}{\sqrt[4]{1 + y^4/y_{\rm max}^4}}\,, \qquad y_{\rm max} = \frac{b_0}{\mu_{\rm min}}$$

Mass effects in splitting DPDs.

[Diehl, Nagar, PP, 2023]

How to treat heavy quarks Q in the small-$\boldsymbol{y}$ DPDs?

Neglecting mass effects:

- Q decouples for $\mu_{\text{spl}} < \gamma m_Q \sim m_Q$.
- Q massless for $\mu_{\text{spl}} > \gamma m_Q \sim m_Q$.

Including mass effects:

- Q decouples for $\mu_{\text{spl}} < \alpha m_Q \ll m_Q$.
- Q massive for $\alpha m_Q < \mu_{\text{spl}} < \beta m_Q$.
- Q massless for $\mu_{\text{spl}} > \beta m_Q \gg m_Q$.

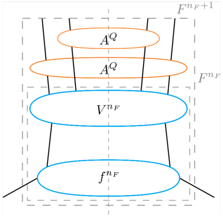

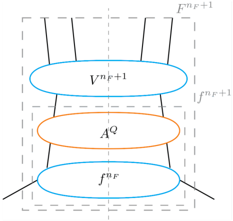

γm_Q $\quad$ μ_{split}

Mass effects in splitting DPDs.

[Diehl, Nagar, PP, 2023]

How to treat heavy quarks Q in the small-y DPDs?

Neglecting mass effects:

- Q decouples for $\mu_{\text{spl}} < \gamma m_Q \sim m_Q$.
- Q massless for $\mu_{\text{spl}} > \gamma m_Q \sim m_Q$.

Including mass effects:

- Q decouples for $\mu_{\text{spl}} < \alpha m_Q \ll m_Q$.
- Q massive for $\alpha m_Q < \mu_{\text{spl}} < \beta m_Q$.
- Q massless for $\mu_{\text{spl}} > \beta m_Q \gg m_Q$.

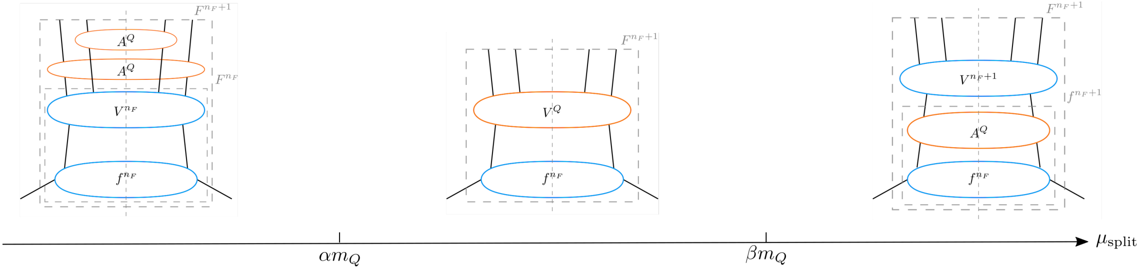

Splitting scale dependence at LO.

In order to estimate the dependence of DPS cross sections on μ_{spl} consider DPD luminosities:

DPS factorization theorem:

$$\sigma^{AB}_{\text{DPS}} = \frac{1}{1+\delta_{AB}} \sum_{a_1,a_2,b_1,b_2} \hat{\sigma}^{A}_{a_1 b_1} \otimes \hat{\sigma}^{B}_{a_2 b_2} \otimes \underbrace{\int_{b_0/\nu}^{\infty} \mathrm{d}^2\boldsymbol{y}\, F_{a_1 a_2}(x_1, x_2, \boldsymbol{y}; Q_A, Q_B)\, F_{b_1 b_2}(\bar{x}_1, \bar{x}_2, \boldsymbol{y}; Q_A, Q_B)}_{\mathcal{L}_{a_1 a_2, b_1 b_2}(x_1, x_2, \bar{x}_1, \bar{x}_2; Q_A, Q_B)}$$

Include factorised model for intrinsic part of DPDs:

$$F^{\text{int}}_{a_1 a_2}(x_1, x_2, \boldsymbol{y}; \mu, \mu) = (1 - \delta^{d_v d_v}_{a_1 a_2} - 0.5\, \delta^{u_v u_v}_{a_1 a_2}) \frac{(1-x_1-x_2)^2}{(1-x_1)^2(1-x_2)^2} \frac{\exp\left(\frac{-\boldsymbol{y}^2}{4h_{a_1 a_2}}\right)}{4\pi h_{a_1 a_2}} f_{a_1}(x_1; \mu) f_{a_2}(x_2; \mu)$$

Contributions to the luminosities: 1v1 (spl $\times$ spl), 1v2 (spl $\times$ int), 2v1 (int $\times$ spl), 2v2 (int $\times$ int).

Splitting scale dependence at LO.

Vary μ_{spl} by a factor of 2 around its central value:

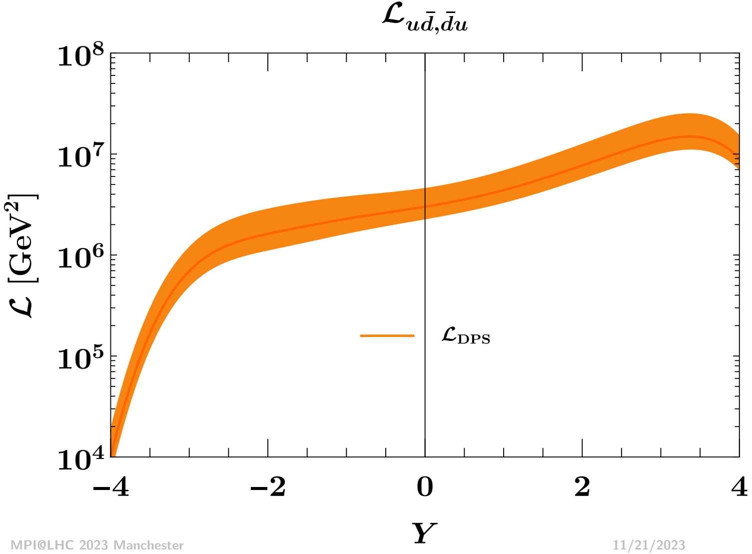

Sum of all contributions to $\mathcal{L}_{u\bar{d},\bar{d}u}(80\,\text{GeV}, 80\,\text{GeV})$ with:

$$x_1 = \frac{Q_A}{\sqrt{s}} e^{Y}$$

$$x_2 = \frac{Q_B}{\sqrt{s}} e^{-Y}$$

$$\bar{x}_1 = \frac{Q_A}{\sqrt{s}} e^{-Y}$$

$$\bar{x}_2 = \frac{Q_B}{\sqrt{s}} e^{Y}$$

where $\sqrt{s} = 14\,\text{GeV}$.

Splitting scale dependence at LO.

Vary μ_{spl} by a factor of 2 around its central value:

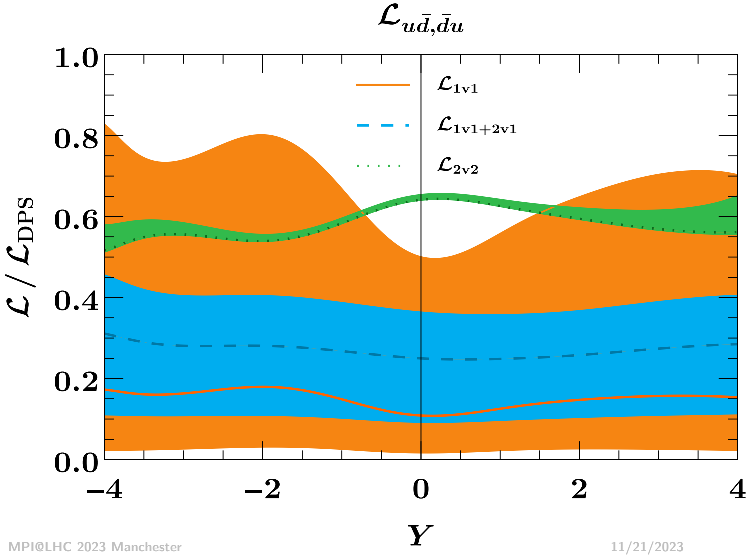

Relative contributions of 1v1, 1v2+2v1, and 2v2 to the complete $\mathcal{L}_{u\bar{d},\bar{d}u}$ luminosity for central ν.

Splitting scale dependence at LO.

Vary μ_{spl} by a factor of 2 around its central value:

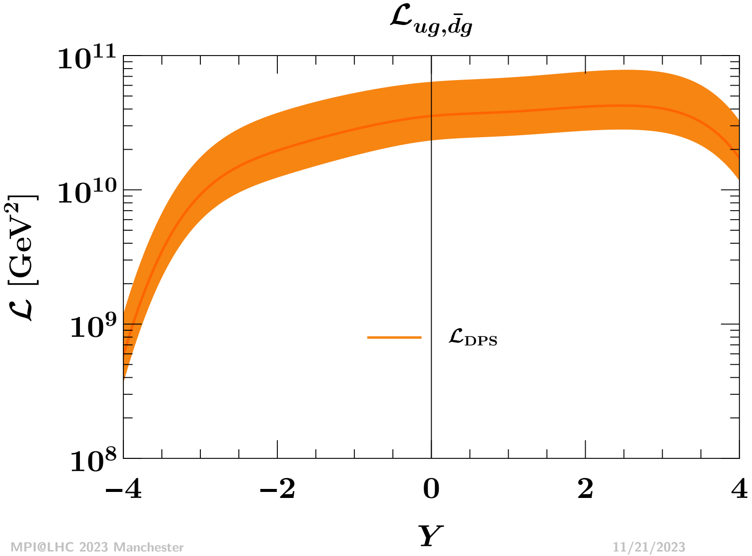

Sum of all contributions to $\mathcal{L}_{ug,\bar{d}g}(80\,\text{GeV}, 25\,\text{GeV})$ with:

$$x_1 = \frac{Q_A}{\sqrt{s}} \mathrm{e}^{Y}$$

$$x_2 = \frac{Q_B}{\sqrt{s}} \mathrm{e}^{-Y}$$

$$\bar{x}_1 = \frac{Q_A}{\sqrt{s}} \mathrm{e}^{-Y}$$

$$\bar{x}_2 = \frac{Q_B}{\sqrt{s}} \mathrm{e}^{Y}$$

where $\sqrt{s} = 14\,\text{GeV}$.

Splitting scale dependence at LO.

Vary $\mu_{\rm spl}$ by a factor of 2 around its central value:

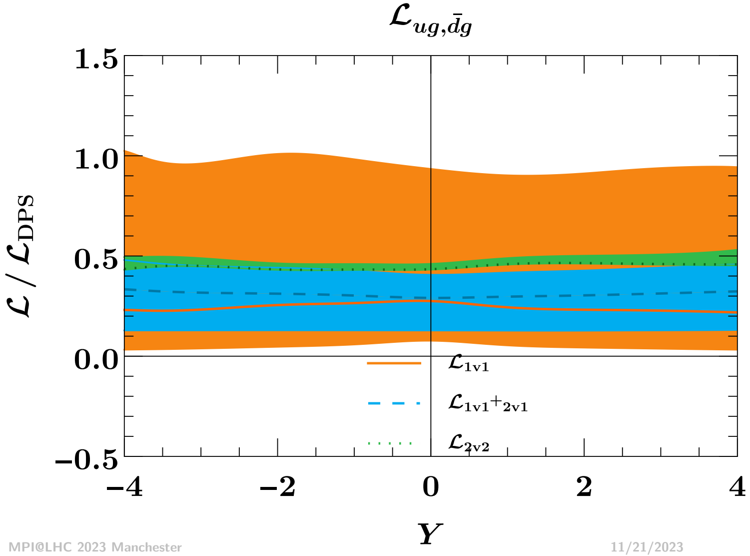

Relative contributions of 1v1, 1v2+2v1, and 2v2 to the complete $\mathcal{L}_{ug,\bar{d}g}$ luminosity for central ν.

Splitting DPDs at NLO.

[Diehl, Gaunt, PP, Schäfer, 2019; Diehl, Gaunt, PP, 2021]

LO splitting DPDs exhibit a huge dependence on μ_{spl}, hinting at the importance of higher orders!

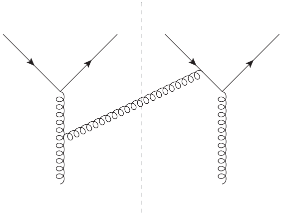

Computation of the NLO $1 \to 2$ splitting kernels ${}^{R_1 R_2}V^{(2)}_{a_1 a_2, a_0}$:

- Bare kernels from two-loop Feynman diagrams for partonic DPDs $a_1 a_2$ in parton a_0.
- Consistent regularization of rapidity divergences.
- Renormalized kernels obtained through RGE analysis.

Structure of NLO kernels:

$$V^{(2)}_{a_1 a_2, a_0}(z_1, z_2, \boldsymbol{y}; \mu, \zeta) = V^{[2,0]}_{a_1 a_2, a_0}(z_1, z_2) + L\, V^{[2,1]}_{a_1 a_2, a_0}(z_1, z_2)$$

where $L = \log \frac{y^2 \mu^2}{b_0^2}$.

State of the art for perturbative splitting DPDs.

At which perturbative orders are the $1 \to 2$ position space splitting kernels known?

	col singlet	col non-singlet
unpol	NLO	NLO
pol	LO	LO

Massless $V_{a_1 a_2, a_0}$ kernels.

	col singlet	col non-singlet
unpol	approx. NLO	LO
pol	LO	LO

Massive $V^{Q}_{a_1 a_2, a_0}$ kernels.

Consider now the impact of including the NLO contributions, focus on the colour singlet!

Part II

NLO numerics.

Numerical evolution with ChiliPDF

[Diehl, Nagar, PP, Tackmann, 2023]

ChiliPDF is a C++ library for the evolution and interpolation of PDFs and position space DPDs!

Design:

- DPDs are discretized in x_1, x_2, and y on Chebyshev grids, allowing for high interpolation accuracy with fewer points than e.g. splines.
- No gridding in μ_1 and μ_2 – evolution is performed on the fly using higher-order Runge-Kutta algorithms.

Features:

- Evolution and flavour matching for DPDs (unpolarized and polarized, colour singlet and non-singlet) at the highest available order.
- Small-y splitting DPDs at NLO.
- Evaluation of sum rules for unpolarized colour singlet DPDs.
- Computation of DPS luminosities.

Numerical implementation of NLO splitting DPDs.

At NLO the splitting DPD no longer is a simple product kernel × PDF, but involves a convolution:

NLO splitting:

$$F^{\text{spl},(2)}_{a_1 a_2}(x_1, x_2, \boldsymbol{y}; \mu, \mu) = \frac{1}{\pi \boldsymbol{y}^2} \left(\frac{\alpha_s(\mu)}{2\pi} \right)^2 \left[V^{(2)}_{a_1 a_2, a_0}(\boldsymbol{y}, \mu) \underset{12}{\otimes} f_{a_0}(\mu) \right] (x_1, x_2)$$

where:

$$x = x_1 + x_2, \qquad u = \frac{x_1}{x}, \qquad \bar{u} = 1 - u = \frac{x_2}{x}$$

How to discretize this convolution?

Numerical implementation of NLO splitting DPDs.

At NLO the splitting DPD no longer is a simple product kernel × PDF, but involves a convolution:

NLO splitting:

$$F^{\text{spl},\,(2)}_{a_1 a_2}(x_1, x_2, \boldsymbol{y}; \mu, \mu) = \frac{1}{\pi \boldsymbol{y}^2} \left(\frac{\alpha_s(\mu)}{2\pi} \right)^2 \int_{x_1+x_2}^{1} \frac{\mathrm{d}z}{z^2} \, V^{(2)}_{a_1 a_2, a_0} \left(\tfrac{x_1}{z}, \tfrac{x_2}{z}, \boldsymbol{y}; \mu \right) f_{a_0}(z; \mu)$$

where:

$$x = x_1 + x_2, \qquad u = \frac{x_1}{x}, \qquad \bar{u} = 1 - u = \frac{x_2}{x}$$

How to discretize this convolution?

Numerical implementation of NLO splitting DPDs.

At NLO the splitting DPD no longer is a simple product kernel × PDF, but involves a convolution:

NLO splitting:

$$F^{\text{spl},\,(2)}_{a_1 a_2}(x_1, x_2, \boldsymbol{y}; \mu, \mu) = \frac{1}{\pi \boldsymbol{y}^2} \left(\frac{\alpha_s(\mu)}{2\pi} \right)^2 \frac{1}{x} \int_x^1 \mathrm{d}z \; V^{(2)}_{a_1 a_2, a_0}(uz, \bar{u}z, \boldsymbol{y}; \mu) \, f_{a_0}\left(\tfrac{x}{z}; \mu\right)$$

where:

$$x = x_1 + x_2, \qquad u = \frac{x_1}{x}, \qquad \bar{u} = 1 - u = \frac{x_2}{x}$$

How to discretize this convolution?

Numerical implementation of NLO splitting DPDs.

In ChiliPDF rescaled PDFs, $xf(x)$, and DPDs, $x_1 x_2 F(x_1, x_2)$ are discretized:

$$x_1 x_2 F^{\text{spl},\,(2)}_{a_1 a_2}(x_1, x_2, \boldsymbol{y}; \mu, \mu) = \frac{1}{\pi \boldsymbol{y}^2} \left(\frac{\alpha_s(\mu)}{2\pi} \right)^2 \int_x^1 \frac{\mathrm{d}z}{z} \left(uz\, \bar{u}z\, V^{(2)}_{a_1 a_2, a_0}(uz, \bar{u}z, \boldsymbol{y}; \mu) \right) \left(\tfrac{x}{z} f_{a_0}\left(\tfrac{x}{z}; \mu \right) \right)$$

R.h.s. has the structure of an ordinary Mellin convolution with an additional parameter u!

Discretizing the convolution:

- Discretize $\left(\tilde{K}_{a_1 a_2, a_0}(u, x)\right)_k$ in u and x:

$$\left(\tilde{K}_{a_1 a_2, a_0}(u, x)\right)_k = \sum_{i,j} \left(\tilde{K}_{a_1 a_2, a_0}\right)^{ij}_k b^i_u(u) b^j_x(x)$$

- Regrid $\sum_k \left(\tilde{K}_{a_1 a_2, a_0}(u, x)\right)_k \tilde{f}^k_{a_0}$ in x_1 and x_2 using Chebyshev interpolation.
- Store the computationally expensive $\left(\tilde{K}_{a_1 a_2, a_0}\right)^{ij}_k$ kernels externally and reuse them.

Note: Starting at NLO the evolution equation for momentum space DPDs contains a convolution term of this form!

Numerical implementation of NLO splitting DPDs.

In ChiliPDF rescaled PDFs, $xf(x)$, and DPDs, $x_1 x_2 F(x_1, x_2)$ are discretized:

$$x_1 x_2 F^{\text{spl},\,(2)}_{a_1 a_2}(x_1, x_2, \boldsymbol{y}; \mu, \mu) = \frac{1}{\pi \boldsymbol{y}^2} \left(\frac{\alpha_s(\mu)}{2\pi} \right)^2 \int_x^1 \frac{\mathrm{d}z}{z}\, \tilde{V}^{(2)}_{a_1 a_2, a_0}(u, z, \boldsymbol{y}; \mu)\, \tilde{f}_{a_0}\left(\tfrac{x}{z}; \mu\right)$$

R.h.s. has the structure of an ordinary Mellin convolution with an additional parameter u!

Discretizing the convolution:

- Discretize $\left(\tilde{K}_{a_1 a_2, a_0}(u, x)\right)_k$ in u and x:

$$\left(\tilde{K}_{a_1 a_2, a_0}(u, x)\right)_k = \sum_{i,j} \left(\tilde{K}_{a_1 a_2, a_0}\right)^{ij}_k b^i_u(u) b^j_x(x)$$

- Regrid $\sum_k \left(\tilde{K}_{a_1 a_2, a_0}(u, x)\right)_k \tilde{f}^k_{a_0}$ in x_1 and x_2 using Chebyshev interpolation.
- Store the computationally expensive $\left(\tilde{K}_{a_1 a_2, a_0}\right)^{ij}_k$ kernels externally and reuse them.

Note: Starting at NLO the evolution equation for momentum space DPDs contains a convolution term of this form!

Numerical implementation of NLO splitting DPDs.

In ChiliPDF rescaled PDFs, $xf(x)$, and DPDs, $x_1 x_2 F(x_1, x_2)$ are discretized:

$$x_1 x_2 F^{\text{spl},\,(2)}_{a_1 a_2}(x_1, x_2, \boldsymbol{y}; \mu, \mu) = \frac{1}{\pi \boldsymbol{y}^2} \left(\frac{\alpha_s(\mu)}{2\pi} \right)^2 \int_x^1 \frac{\mathrm{d}z}{z} \, \tilde{V}^{(2)}_{a_1 a_2, a_0}(u, z, \boldsymbol{y}; \mu) \sum_k \tilde{f}^k_{a_0}(\mu)\, b^k\left(\tfrac{x}{z}\right)$$

R.h.s. has the structure of an ordinary Mellin convolution with an additional parameter u!

Discretizing the convolution:

- Discretize $\left(\tilde{K}_{a_1 a_2, a_0}(u, x)\right)_k$ in u and x:

$$\left(\tilde{K}_{a_1 a_2, a_0}(u, x)\right)_k = \sum_{i,j} \left(\tilde{K}_{a_1 a_2, a_0}\right)^{ij}_k b^i_u(u) b^j_x(x)$$

- Regrid $\sum_k \left(\tilde{K}_{a_1 a_2, a_0}(u, x)\right)_k \tilde{f}^k_{a_0}$ in x_1 and x_2 using Chebyshev interpolation.
- Store the computationally expensive $\left(\tilde{K}_{a_1 a_2, a_0}\right)^{ij}_k$ kernels externally and reuse them.

Note: Starting at NLO the evolution equation for momentum space DPDs contains a convolution term of this form!

Numerical implementation of NLO splitting DPDs.

In `ChiliPDF` rescaled PDFs, $xf(x)$, and DPDs, $x_1 x_2 F(x_1, x_2)$ are discretized:

$$x_1 x_2 F^{\text{spl},\,(2)}_{a_1 a_2}(x_1, x_2, \boldsymbol{y}; \mu, \mu) = \frac{1}{\pi \boldsymbol{y}^2} \left(\frac{\alpha_s(\mu)}{2\pi} \right)^2 \sum_k \left(\tilde{K}_{a_1 a_2, a_0}(u, x, \boldsymbol{y}; \mu) \right)_k \tilde{f}^k_{a_0}(\mu)$$

R.h.s. has the structure of an ordinary Mellin convolution with an additional parameter u!

Discretizing the convolution:

- Discretize $\left(\tilde{K}_{a_1 a_2, a_0}(u, x)\right)_k$ in u and x:

$$\left(\tilde{K}_{a_1 a_2, a_0}(u, x)\right)_k = \sum_{i,j} \left(\tilde{K}_{a_1 a_2, a_0}\right)^{ij}_k b^i_u(u) b^j_x(x)$$

- Regrid $\sum_k \left(\tilde{K}_{a_1 a_2, a_0}(u, x)\right)_k \tilde{f}^k_{a_0}$ in x_1 and x_2 using Chebyshev interpolation.
- Store the computationally expensive $\left(\tilde{K}_{a_1 a_2, a_0}\right)^{ij}_k$ kernels externally and reuse them.

Note: Starting at NLO the evolution equation for momentum space DPDs contains a convolution term of this form!

Numerical setup

For the study of the massless and massive $1 \to 2$ splitting at NLO the following setup is used:

PDFs:

- PDF set for LO splitting: `MSHT20lo_as130`.
- PDF set for NLO splitting: `MSHT20nlo_as118`.

Grids:

- Same grids for x_1 and x_2: $\left[10^{-5}, 0.005, 0.5, 1\right]_{(16,16,24)}$.
- y-grid for massless splitting: $\left[\frac{b_0}{2\min(Q_A,Q_B)}, \frac{b_0}{m_b}, \frac{b_0}{m_c}, 5, \infty\right]_{(16,16,16,24)}$.
- y-grid for massive splitting: $\left[\frac{b_0}{2\min(Q_A,Q_B)}, \frac{b_0}{\beta\, m_b}, \frac{b_0}{\beta\, m_c}, \frac{b_0}{\alpha\, m_b}, 5, \infty\right]_{(16,16,16,16,24)}$.

Various parameters:

- $\mu_{\min} = m_c$.
- $h_{gg} = 4.66\,\mathrm{GeV}^{-1}$, $h_{qg} = 5.86\,\mathrm{GeV}^{-1}$, $h_{qq} = 7.06\,\mathrm{GeV}^{-1}$.

Splitting DPDs at LO and NLO.

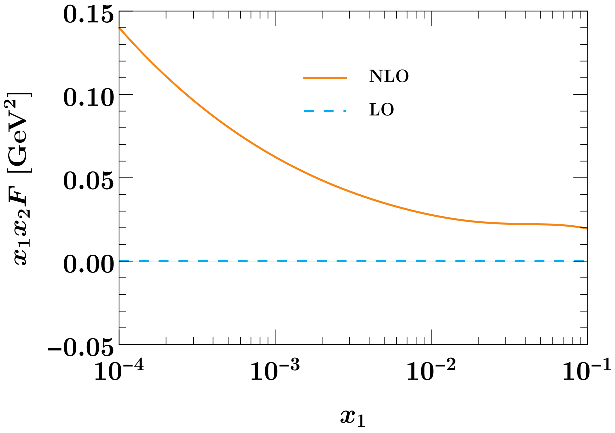

Figure: $F^{\text{spl}}_{u\bar{d}}$ at $(\mu_1, \mu_2) = (80\,\text{GeV}, 80\,\text{GeV})$ and $y = \frac{b_0}{80\,\text{GeV}}$ for $x_1 = x_2$ as a function of x_1. Relevant in W^+W^+ production.

- At LO $F_{u\bar{d}}$ is not produced by splitting, only through evolution.
- Starting from NLO $F_{u\bar{d}}$ can be produced by splitting.
- The NLO splitting mechanism is the leading contribution.

Splitting DPDs at LO and NLO.

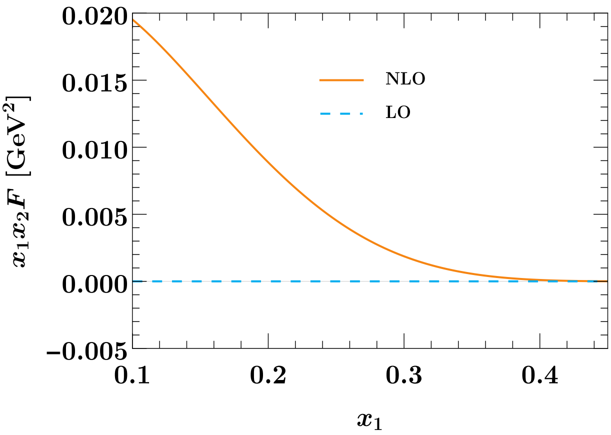

Figure: $F^{\text{spl}}_{u\bar{d}}$ at $(\mu_1, \mu_2) = (80\,\text{GeV}, 80\,\text{GeV})$ and $y = \frac{b_0}{80\,\text{GeV}}$ for $x_1 = x_2$ as a function of x_1. Relevant in W^+W^+ production.

- At LO $F_{u\bar{d}}$ is not produced by splitting, only through evolution.
- Starting from NLO $F_{u\bar{d}}$ can be produced by splitting.
- The NLO splitting mechanism is the leading contribution.

Splitting DPDs at LO and NLO.

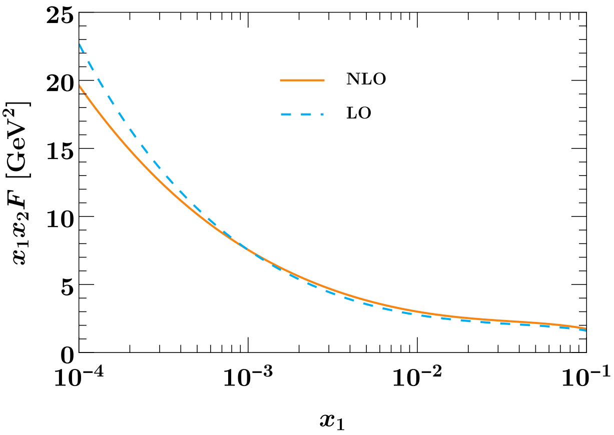

Figure: F_{ug}^{spl} at $(\mu_1, \mu_2) = (80\,\text{GeV}, 25\,\text{GeV})$ and $y = \frac{b_0}{80\,\text{GeV}}$ for $x_1 = x_2$ as a function of x_1. Relevant in $W^+ +$ jet production.

- F_{ug} is already produced by splitting at LO.
- The difference between LO and NLO is non-negligible ($\mathcal{O}(10\%)$).

Splitting DPDs at LO and NLO.

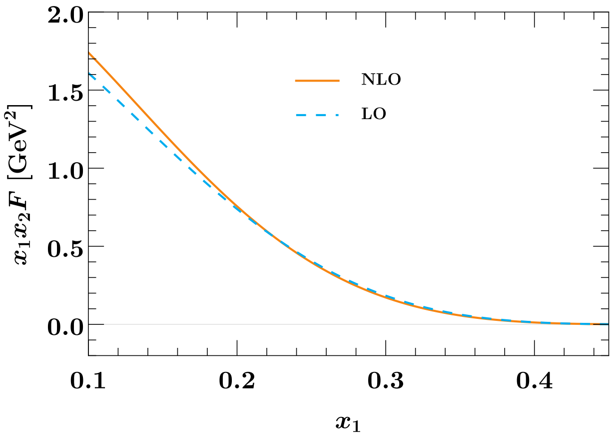

Figure: F_{ug}^{spl} at $(\mu_1, \mu_2) = (80\,\mathrm{GeV}, 25\,\mathrm{GeV})$ and $y = \frac{b_0}{80\,\mathrm{GeV}}$ for $x_1 = x_2$ as a function of x_1. Relevant in $W^+ +$ jet production.

- F_{ug} is already produced by splitting at LO.
- The difference between LO and NLO is non-negligible ($\mathcal{O}(10\%)$).

DPD luminosities at LO and NLO: splitting scale dependence.

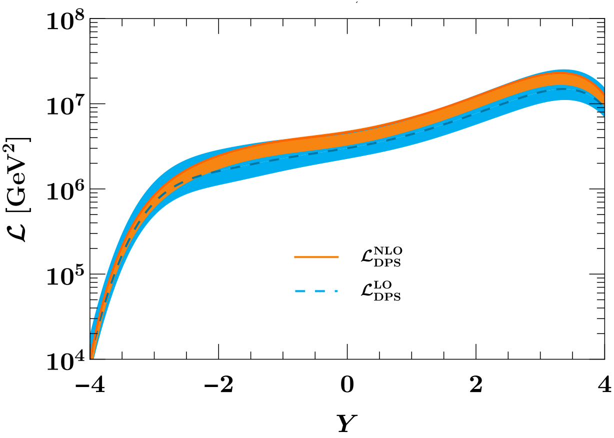

Figure: Splitting scale dependence of $\mathcal{L}_{u\bar{d},\bar{d}u}(80\,\mathrm{GeV}, 80\,\mathrm{GeV})$ at LO and NLO. Relevant for W^+W^+ production.

- From LO to NLO the splitting scale dependence of $\mathcal{L}_{u\bar{d},\bar{d}u}$ is reduced by a factor of $\sim$2 for all rapidities.
- As expected, this reduction is most pronounced for the 1v1 contribution.

DPD luminosities at LO and NLO: splitting scale dependence.

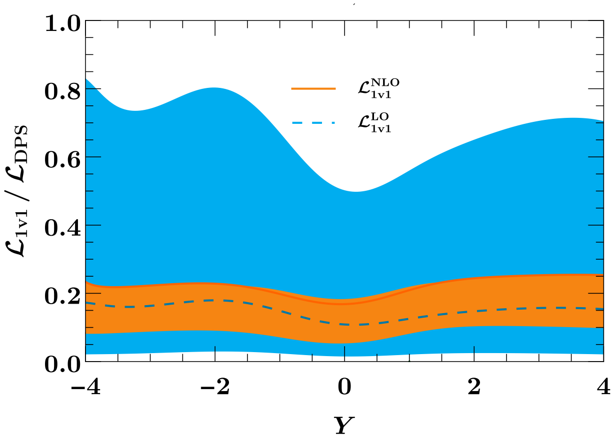

Figure: Splitting scale dependence of the (relative) 1v1 contribution to $\mathcal{L}_{u\bar{d},\bar{d}u}(80\,\mathrm{GeV}, 80\,\mathrm{GeV})$ at LO and NLO.

- From LO to NLO the splitting scale dependence of $\mathcal{L}_{u\bar{d},\bar{d}u}$ is reduced by a factor of $\sim$2 for all rapidities.
- As expected, this reduction is most pronounced for the 1v1 contribution.

DPD luminosities at LO and NLO: splitting scale dependence.

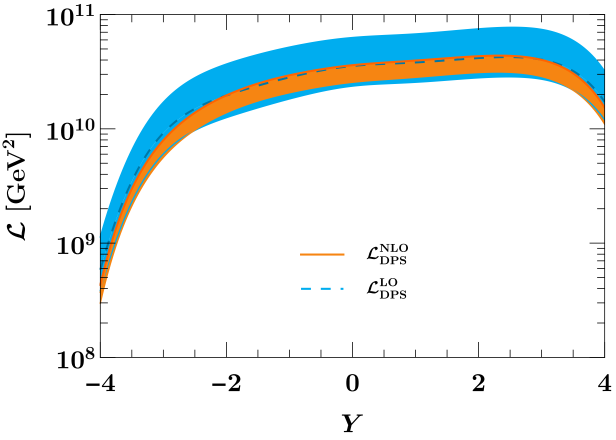

Figure: Splitting scale dependence of $\mathcal{L}_{ug,\bar{d}g}(80\,\mathrm{GeV}, 25\,\mathrm{GeV})$ at LO and NLO. Relevant for $W^+ +$ jet production.

- For $\mathcal{L}_{ug,\bar{d}g}$ the splitting scale dependence is reduced by more than a factor of 2 for all rapidities, when going from LO to NLO.
- The largest reduction is again observed for the 1v1 contribution.

Similar reduction observed in other channels and for colour non-singlet luminosities!

Sizeable reduction also for the remnant cut-off scale dependence!

DPD luminosities at LO and NLO: splitting scale dependence.

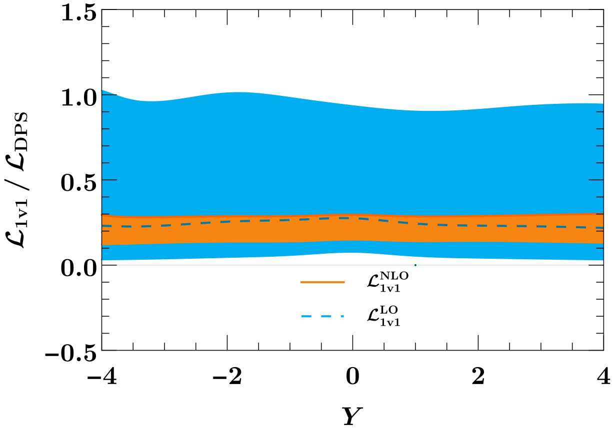

Figure: Splitting scale dependence of the (relative) 1v1 contribution to $\mathcal{L}_{ug,\bar{d}g}(80\,\text{GeV}, 25\,\text{GeV})$ at LO and NLO.

- For $\mathcal{L}_{ug,\bar{d}g}$ the splitting scale dependence is reduced by more than a factor of 2 for all rapidities, when going from LO to NLO.
- The largest reduction is again observed for the 1v1 contribution.

Similar reduction observed in other channels and for colour non-singlet luminosities!

Sizeable reduction also for the remnant cut-off scale dependence!

Massive splitting scheme: Issues at LO.

In the massive splitting scheme α and β should be $\ll 1$ and $\gg 1$, respectively. Issue at LO:

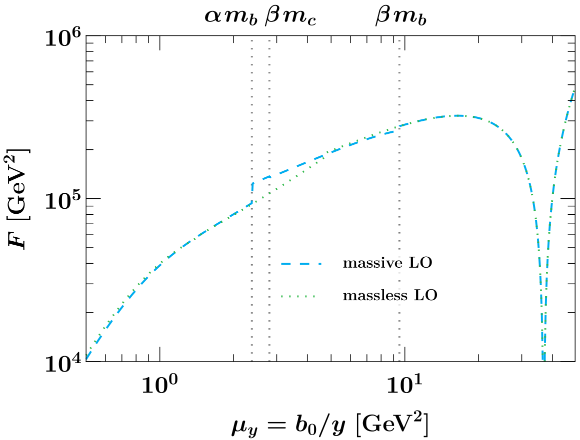

- Going to smaller α decreases the absolute size of the discontinuity.
- Going to $\beta \gtrsim 2$ is not possible due to a large discontinuity that arises in this limit.
- How does this discontinuity arise?

Figure: F_{gb}^{spl} at $\mu_{1,2} = 25\,\mathrm{GeV}$ with $x_{1,2} \approx 0.0018$ as function of $\mu_y = b_0/y$.

Massive splitting scheme: Issues at LO.

In the massive splitting scheme α and β should be $\ll 1$ and $\gg 1$, respectively. Issue at LO:

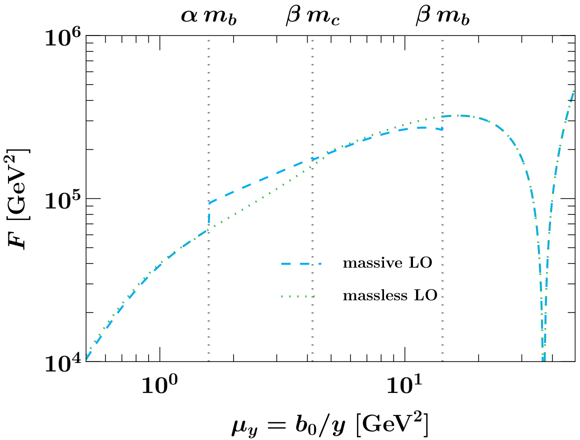

- Going to smaller α decreases the absolute size of the discontinuity.
- Going to $\beta \gtrsim 2$ is not possible due to a large discontinuity that arises in this limit.
- How does this discontinuity arise?

Figure: F_{gb}^{spl} at $\mu_{1,2} = 25\,\text{GeV}$ with $x_{1,2} \approx 0.0018$ as function of $\mu_y = b_0/y$.

Massive splitting scheme: Issues at LO.

In the massive splitting scheme α and β should be $\ll 1$ and $\gg 1$, respectively. Issue at LO:

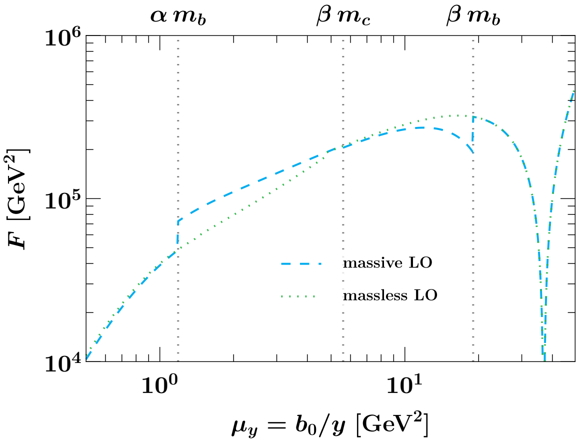

- Going to smaller α decreases the absolute size of the discontinuity.
- Going to $\beta \gtrsim 2$ is not possible due to a large discontinuity that arises in this limit.
- How does this discontinuity arise?

Figure: F_{gb}^{spl} at $\mu_{1,2} = 25\,\mathrm{GeV}$ with $x_{1,2} \approx 0.0018$ as function of $\mu_y = b_0/y$.

Massive splitting scheme: Issues at LO.

Consider now how the gb DPD can be produced in the different schemes:

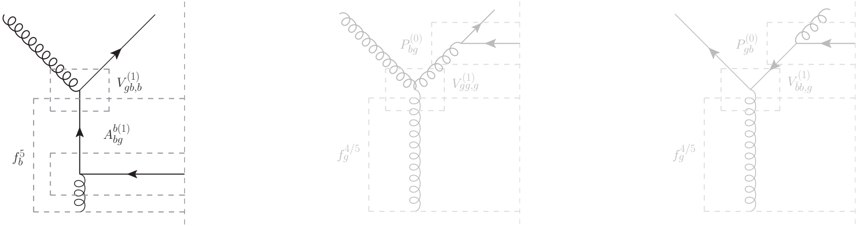

- The direct $b \to gb$ splitting is only accessible in the massless scheme.
- The b PDF is obtained by flavour matching from a $n_F = 4$ gluon PDF.
- At NLO this production channel becomes available also in the massive scheme!

Massive splitting scheme: Issues at LO.

Consider now how the gb DPD can be produced in the different schemes:

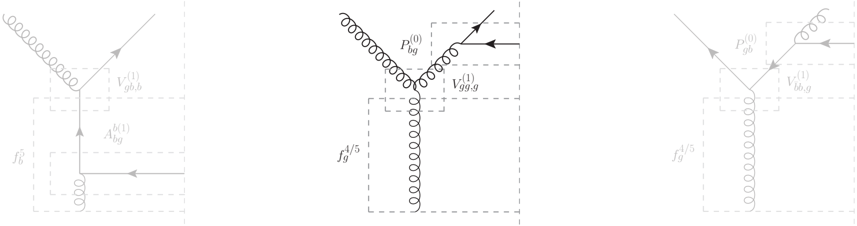

- This production channel, involving one evolution step, is accessible both in the massive and massless schemes.
- In the massless scheme the initial gluon PDF is a $n_F = 5$ distribution, whereas in the massive scheme it is $n_F = 4$.

Massive splitting scheme: Issues at LO.

Consider now how the gb DPD can be produced in the different schemes:

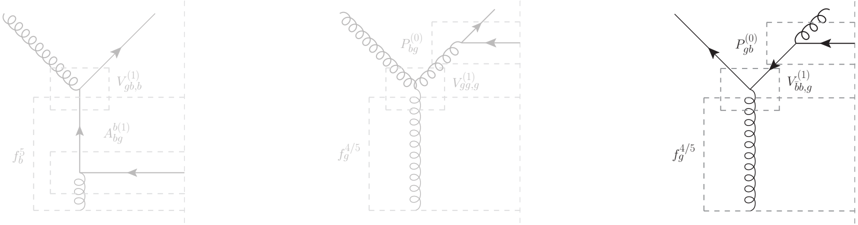

- This production channel, involving one evolution step, is accessible both in the massive and massless schemes.
- In the massless scheme the initial gluon PDF is a $n_F = 5$ distribution, whereas in the massive scheme it is $n_F = 4$.
- In the massive scheme the massive $g \to b\bar{b}$ kernel is used.

Massive splitting scheme: Issues at LO.

In the massive splitting scheme α and β should be $\ll 1$ and $\gg 1$, respectively. No more issue at NLO:

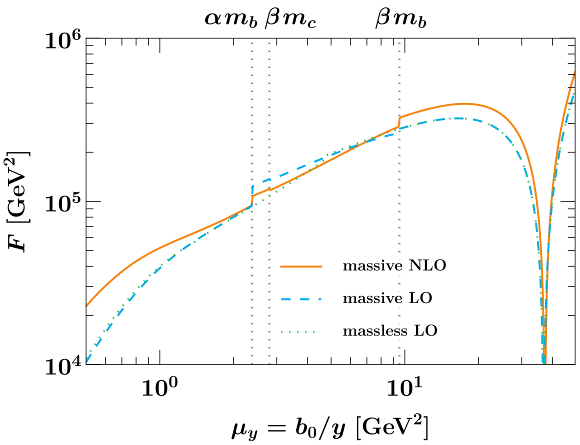

Figure: F_{gb}^{spl} at $\mu_{1,2} = 25\,\text{GeV}$ with $x_{1,2} \approx 0.0018$ as function of $\mu_y = b_0/y$.

- Going to smaller α decreases the absolute size of the discontinuity.
- Unfortunately going to $\beta \gtrsim 2$ is not possible due to a large discontinuity that arises in this limit.
- Going to NLO avoids this discontinuity!

Massive splitting scheme: Issues at LO.

In the massive splitting scheme α and β should be $\ll 1$ and $\gg 1$, respectively. No more issue at NLO:

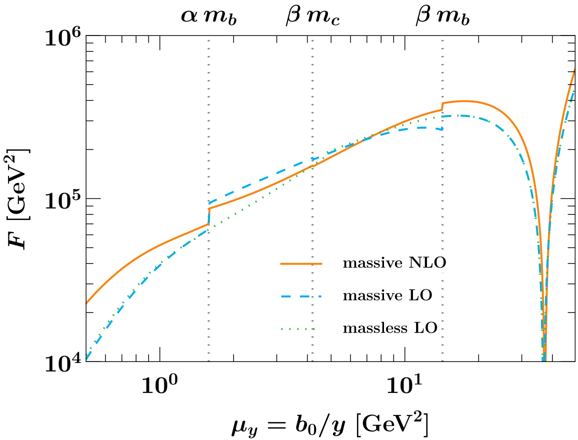

- Going to smaller α decreases the absolute size of the discontinuity.
- Unfortunately going to $\beta \gtrsim 2$ is not possible due to a large discontinuity that arises in this limit.
- Going to NLO avoids this discontinuity!

Figure: F_{gb}^{spl} at $\mu_{1,2} = 25\,\text{GeV}$ with $x_{1,2} \approx 0.0018$ as function of $\mu_y = b_0/y$.

Massive splitting scheme: Issues at LO.

In the massive splitting scheme α and β should be $\ll 1$ and $\gg 1$, respectively. No more issue at NLO:

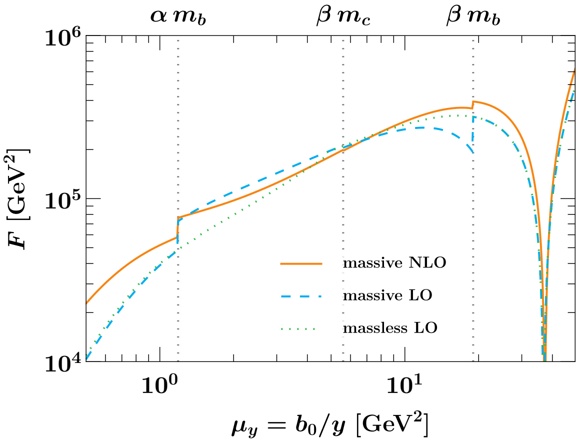

- Going to smaller α decreases the absolute size of the discontinuity.
- Unfortunately going to $\beta \gtrsim 2$ is not possible due to a large discontinuity that arises in this limit.
- Going to NLO avoids this discontinuity!

Figure: F_{gb}^{spl} at $\mu_{1,2} = 25\,\mathrm{GeV}$ with $x_{1,2} \approx 0.0018$ as function of $\mu_y = b_0/y$.

Part III

Summary.

Summary.

State of the art for small interparton distance splitting DPDs:

- NLO for unpolarized massless colour singlet and non-singlet kernels.
- Approximate NLO for unpolarized massive colour singlet kernels.
- LO for all other cases.

Effects of going to NLO:

- $\mathcal{O}(10\%)$ for DPDs produced already by LO splitting.
- Leading contribution for DPDs not directly produced by LO splitting.
- Substantial reduction of scale uncertainty related to the splitting scale μ_{spl}.
- Sizeable reduction of the remnant dependence on the DGS cut-off scale ν.
- More consistent treatment of heavy quark effects in the perturbative splitting.

Summary.

State of the art for small interparton distance splitting DPDs:

- NLO for unpolarized massless colour singlet and non-singlet kernels.
- Approximate NLO for unpolarized massive colour singlet kernels.
- LO for all other cases.

Effects of going to NLO:

- $\mathcal{O}(10\%)$ for DPDs produced already by LO splitting.
- Leading contribution for DPDs not directly produced by LO splitting.
- Substantial reduction of scale uncertainty related to the splitting scale μ_{spl}.
- Sizeable reduction of the remnant dependence on the DGS cut-off scale ν.
- More consistent treatment of heavy quark effects in the perturbative splitting.

Thank you for your attention!

Part IV

Backup.

Small distance limit of DPDs.

Diehl-Gaunt-Schönwald subtraction formalism: basic idea.

[Diehl, Gaunt, Schönwald, 2017]

Avoid double counting between SPS and DPS by introducing a subtraction term satisfying:

DGS subtraction term:

$$\frac{\mathrm{d}\sigma_{\mathrm{sub}}}{\mathrm{d}y} \xrightarrow{y\to 0} \frac{\mathrm{d}\sigma_{\mathrm{DPS}}}{\mathrm{d}y}\,, \qquad \frac{\mathrm{d}\sigma_{\mathrm{sub}}}{\mathrm{d}y} \xrightarrow{y\to \infty} \frac{\mathrm{d}\sigma_{\mathrm{SPS}}}{\mathrm{d}y}$$

This is achieved by replacing the DPS luminosity in the factorized cross section by:

$$\mathcal{L}^{\mathrm{sub}}_{a_1 a_2, b_1 b_2} = 2\pi \int_{b_0/\nu}^{\infty} \mathrm{d}y\, y\, F^{\mathrm{spl,FO}}_{a_1 a_2}(y; \mu(y, Q_A, \mu_h), \mu(y, Q_B, \mu_h)) F^{\mathrm{spl,FO}}_{b_1 b_2}(y; \mu(y, Q_A, \mu_h), \mu(y, Q_B, \mu_h))$$

where the splitting DPDs are computed at FO with:

$$\mu(y, Q, \mu_h) \xrightarrow{y\to 0} Q\,, \qquad \mu(y, Q, \mu_h) \xrightarrow{y\to \infty} \mu_h\,.$$

How to treat the case $Q_A \neq Q_B$ where the subtraction term is not a pure FO quantity?

Diehl-Gaunt-Schönwald subtraction formalism: unequal scales.

Instead of using profile scales $\mu(y, Q, \mu_h)$ define two sets of DPDs:

- $F^{\text{large}\, y}(y) = F^{\text{spl,FO}}(y; \mu_h, \mu_h)$.
- $F^{\text{small}\, y}(y)$ obtained from evolving $F^{\text{spl,FO}}(y; \nu, \nu)$ to the scales $(\mu_1, \mu_2) = (Q_A, Q_B)$.

Unequal scale DGS subtraction:

$$\mathcal{L}^{\text{sub}}_{a_1 a_2, b_1 b_2} = 2\pi \int_{b_0/\nu}^{\infty} \mathrm{d}y\, y \left[\sigma(y\nu)\, F^{\text{large}\, y}(y)\, F^{\text{large}\, y}(y) + \big(1 - \sigma(y\nu)\big)\, F^{\text{small}\, y}(y)\, F^{\text{small}\, y}(y)\right]$$

with a function $\sigma(u)$ that interpolates smoothly between 0 at $u \sim 1$ and 1 at $u \gg 1$, i.e.:

$$\sigma(u) = \begin{cases} 0 & \text{for} \quad u < u_0, \\ \sin^2\left(\frac{\pi}{2}\, \frac{u - u_0}{u_1 - u_0}\right) & \text{for} \quad u_0 < u < u_1, \\ 1 & \text{for} \quad u > u_1. \end{cases}$$

DPD luminosities at LO and NLO: cut-off scale dependence.

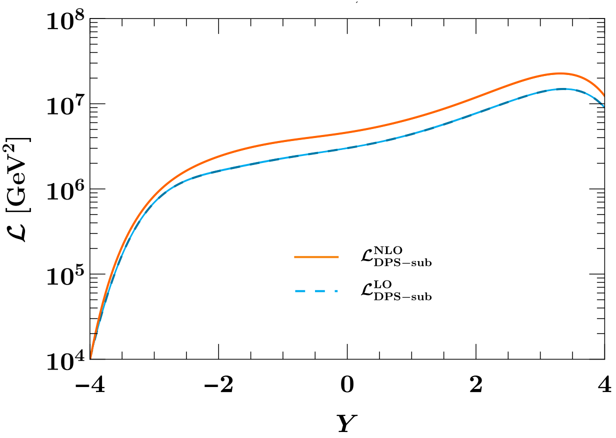

- The subtracted $\mathcal{L}_{u\bar{d},\bar{d}u}$ luminosity exhibits little dependence on the cut-off scale already at LO.
- The cut-off scale dependence of the subtracted 1v1 contribution is noticably reduced from LO to NLO.

Figure: Cut-off scale dependence of the subtracted luminosity $\mathcal{L}_{u\bar{d},\bar{d}u}(80\,\mathrm{GeV}, 80\,\mathrm{GeV})$ at LO and NLO.

DPD luminosities at LO and NLO: cut-off scale dependence.

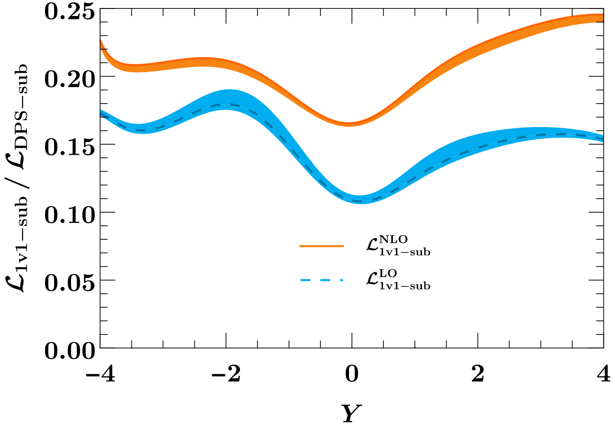

Figure: Cut-off scale dependence of the (relative) subtracted 1v1 contribution to $\mathcal{L}_{u\bar{d},\bar{d}u}(80\,\mathrm{GeV}, 80\,\mathrm{GeV})$ at LO and NLO.

- The subtracted $\mathcal{L}_{u\bar{d},\bar{d}u}$ luminosity exhibits little dependence on the cut-off scale already at LO.
- The cut-off scale dependence of the subtracted 1v1 contribution is noticably reduced from LO to NLO.

DPD luminosities at LO and NLO: cut-off scale dependence.

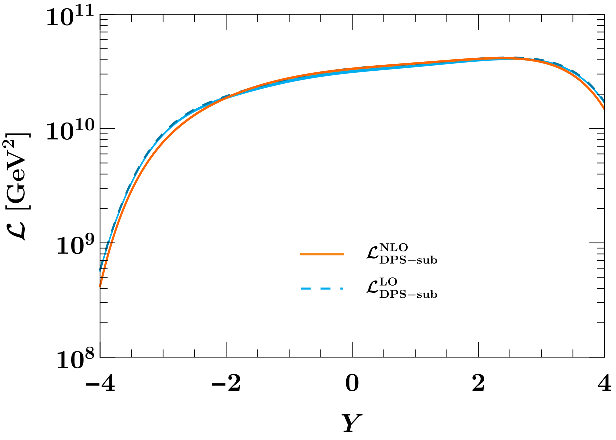

Figure: Cut-off scale dependence of the subtracted luminosity $\mathcal{L}_{ug,\bar{d}g}(80\,\mathrm{GeV}, 25\,\mathrm{GeV})$ at LO and NLO.

- For the subtracted $\mathcal{L}_{ug,\bar{d}g}$ luminosity the remnant cut-off scale dependence is rather small already at LO.
- At NLO this is further reduced, especially for central rapidities.

Similar reduction observed in other channels and for colour non-singlet luminosities!

Except ...

DPD luminosities at LO and NLO: cut-off scale dependence.

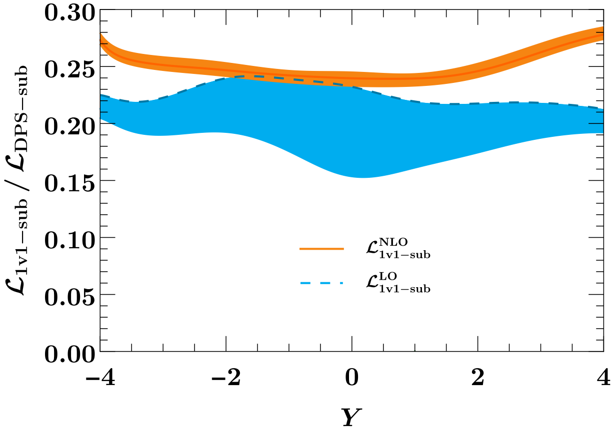

Figure: Cut-off scale dependence of the (relative) subtracted 1v1 contribution to $\mathcal{L}_{ug,\bar{d}g}(80\,\mathrm{GeV}, 25\,\mathrm{GeV})$ at LO and NLO.

- For the subtracted $\mathcal{L}_{ug,\bar{d}g}$ luminosity the remnant cut-off scale dependence is rather small already at LO.
- At NLO this is further reduced, especially for central rapidities.

Similar reduction observed in other channels and for colour non-singlet luminosities!

Except ...

DPD luminosities at LO and NLO: cut-off scale dependence.

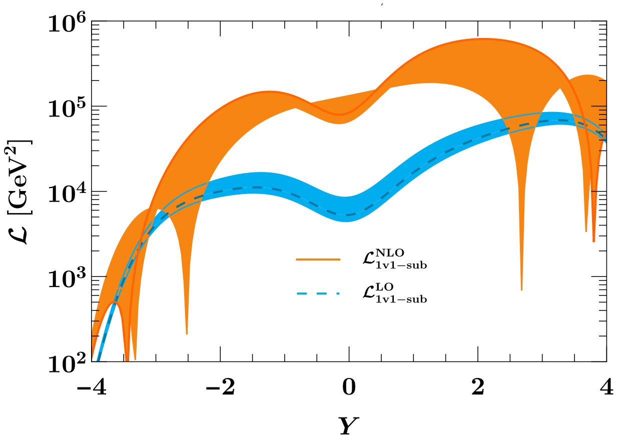

- In this case the cut-off scale dependence increases from LO to NLO.
- Most likely due to absence of Sudakov suppression in the large NLO subtraction term.
- Expect that the dependence decreases at NNLO (subtraction term only starts at NLO).

Figure: Cut-off scale dependence of the subtracted colour octet luminosity ${}^{88,88}\mathcal{L}_{u\bar{d},\bar{d},u}(80\,\text{GeV}, 80\,\text{GeV})$ at LO and NLO.

DPD luminosities at LO and NLO: cut-off scale dependence.

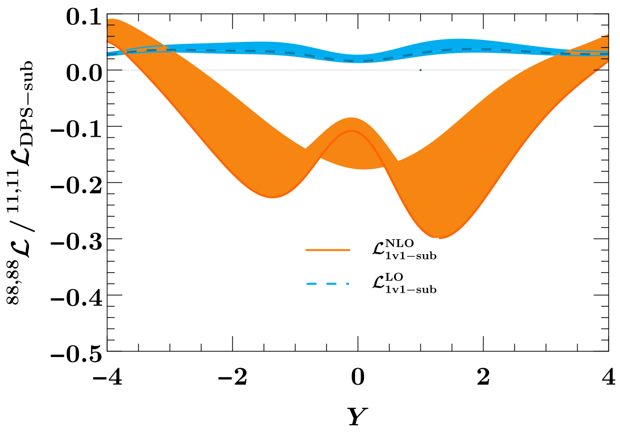

Figure: Cut-off scale dependence of the (relative) subtracted 1v1 contribution to $^{88,88}\mathcal{L}_{u\bar{d},\bar{d},u}(80\,\mathrm{GeV}, 80\,\mathrm{GeV})$ at LO and NLO.

- In this case the cut-off scale dependence increases from LO to NLO.
- Most likely due to absence of Sudakov suppression in the large NLO subtraction term.
- Expect that the dependence decreases at NNLO (subtraction term only starts at NLO).

Cut-off scale dependence in the colour non-singlet.

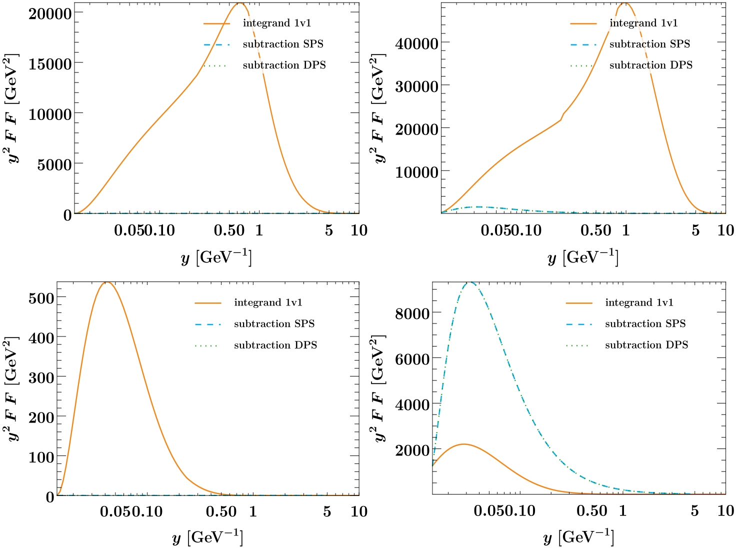

- In the singlet the subtraction term becomes non-zero at NLO(right).
- It stays small compared to the 1v1 term.

- In the non-singlet the 1v1 term is strongly Sudakov suppressed.
- No such suppression is present for the non-zero subtraction term at NLO!